

NASA TM X-56022

FLIGHT EXPERIENCE WITH A PIVOTING TRAVERSING BOUNDARY-LAYER PROBE

Lawrence C. Montoya, David A. Brauns, and Ralph E. Cissell

January 1974

NASA Flight Research Center  
Edwards, California 93523

# FLIGHT EXPERIENCE WITH A PIVOTING TRAVERSING BOUNDARY-LAYER PROBE

Lawrence C. Montoya, David A. Brauns, and Ralph E. Cissell  
Flight Research Center

## ABSTRACT

A pivoting traversing boundary-layer probe was evaluated in flight on an F-104 airplane. The evaluation was performed at free-stream Mach numbers from 0.8 to 2.0. The unit is described, and operating problems and their solutions are discussed. Conventional boundary-layer profiles containing variations in flow angle within the viscous layer are shown for free-stream Mach numbers of 0.8, 1.6, and 2.0. Although the unit was not optimized for size and weight, it successfully measured simultaneously flow angularity, probe height, and pitot pressure through the boundary layer.

## INTRODUCTION

Traversing probes have been shown to be a practical means of improving the definition of boundary layers and wakes (refs. 1 to 6) in a full-scale flight environment. The main advantage of using traversing probes is the relatively small number of sensors and recording channels required to obtain a well-defined boundary-layer profile.

The device used in this investigation was identical to the screw-driven traversing probe tested in the study of reference 5 except that the pitot element was replaced by a unit which pointed into the local airstream as well as traversed the boundary layer. As formerly, the pitot pressure and pitot probe distance from the surface were measured and recorded, but, in addition, the local flow angle was measured and recorded. This paper describes the flight experience with this modified device. As in reference 5, the design effort was not to optimize the size or weight of the device, but to develop a prototype for flight evaluation. Drawings and photographs are presented, and the major problems encountered during the development and testing are discussed.

Typical boundary-layer data obtained on a flight-test fixture, which was fitted on an F-104 airplane at the NASA Flight Research Center, are presented to demonstrate the capabilities of the pivoting traversing probe. The flight data are for free-stream Mach numbers of 0.8, 1.6, and 2.0.

## SYMBOLS

Physical quantities in this report are given in the International System of Units (SI) and parenthetically in U.S. Customary Units. The measurements were taken in U.S. Customary Units. Factors relating the two systems are presented in reference 7.

M	free-stream Mach number
u	local velocity
y	distance from skin
$\psi$	probe angle (see fig. 3)

### Subscript:

e	edge conditions
---	-----------------

## AIRPLANE AND TEST CONDITIONS

An F-104 airplane fitted with an auxiliary ventral fin (flight-test fixture) was used to obtain turbulent compressible boundary layers to demonstrate the performance of the pivoting traversing probe. Figure 1 is a sketch of the airplane with the flight-test fixture installed. The pivoting traversing probe surveyed boundary-layer conditions on the right side of the flight-test fixture 121 centimeters (48 inches) back from the leading edge and 30 centimeters (12 inches) from the airplane fuselage (fig. 2).

The flight-test conditions of this study were free-stream Mach numbers of 0.80, 1.6, and 2.0 at altitudes between 10.06 kilometers (33,000 feet) and 14.63 kilometers (48,000 feet). Each test started and ended with a period of stabilized flight. A gentle longitudinal maneuver (pushdown-pullup) was performed between the stabilized portions to obtain an angle-of-attack excursion of about  $\pm 5^\circ$ .

## EXTERNAL INSTALLATION DETAILS

The three-view sketch of the flight-test fixture in figure 2 shows the location of the pivoting traversing probe. A boundary-layer trip was used to insure a nearly

fixed length of turbulent flow. Figure 3 shows the pivoting traversing probe installation with the fixed surface impact reference probe and flush static orifice. The gaps and screwheads around the pivoting traversing probe were filled and the surface smoothed before each data flight.

## INSTRUMENTATION

All the instrumentation was located within the flight-test fixture, with electrical power supplied by the airplane. The surface impact pressures sensed by the reference probe and the measured static orifice pressures were recorded on a NASA photorecording manometer. The pivoting traversing probe impact pressure was measured on a separate transducer, which was located as close to the sensor as practical, and recorded on tape. The probe height and angle positions were measured with a counter and rotary potentiometer, respectively, and recorded on tape. Pressure lag was considered negligible for this study; a theoretical calculation made using reference 8 estimated the largest lag to be approximately 0.001 second.

### PIVOTING TRAVERSING PROBE

The drive unit for the pivoting traversing probe and the method of measuring probe height is described in detail in reference 5. The unit used in reference 5 was modified slightly for use in the present study. The main differences were in the probe head, probe mast (nonrotating shaft), and probe mast mounting to the drive block; in addition, a potentiometer was added to measure probe rotation. Figure 4 is a photograph of the complete pivoting traversing probe unit and a closeup of the drive block, potentiometer, and some of the other modified parts.

A schematic drawing showing how the parts of the probe were integrated and mounted onto the drive block is presented in figure 5. The probe head was mounted onto the rotating shaft which extended to the drive block within the nonrotating shaft. Both shafts were then supported on the drive block with a collar. A potentiometer with a hollow shaft, made especially for this application, was mounted on the underside of the drive block with its shaft extending through the drive block into the rotating shaft. An O-ring was used to form a pressure seal between the rotating potentiometer shaft and the rotating probe shaft. Flexible tubing was then attached between the potentiometer shaft and pressure sensor. Thus probe rotation and pressure measurements could be transmitted continuously from the probe head to the position potentiometer and pressure sensor.

A photograph and detailed dimensions of the probe head are shown in figure 6. The probe tail fins were configured such that they were the same thickness and in the same plane as the probe head. This arrangement was used so that flow-direction measurements would represent the measured pressure plane. During assembly, the probe was mass balanced on the rotating shaft to reduce inertia effects. The rotating shaft itself was threaded approximately 2.54 centimeters (1 inch) below the probe so

that the probe head could be removed to disassemble the unit (fig. 5).

The maximum traverse of the probe from the surface for this application was approximately 6.1 centimeters (2.4 inches), with an angular throw of  $\pm 30^\circ$ . The traversing rate was approximately 0.8 cm/sec (0.3 in/sec).

## OPERATING PROBLEMS

Problems encountered during development and testing of the modified portions of the unit and the methods used to alleviate them are discussed in this section.

### Rotation Resistance

A major concern during construction of the pivoting traversing probe was to keep the rotational resistance of the probe as low as possible. This was desirable because the flow energy within the lower portions of the boundary layer tends to be low, making flow angularity measurements with a vane system difficult.

The two main components of rotational resistance consisted of friction resistance between parts and the resistance due to the flexible tubing weight and stiffness.<sup>1</sup> The friction resistance between parts was alleviated by maintaining very close tolerances, alinement, and smooth surface finish between parts.

The flexible tubing rotational resistance was alleviated by using 0.318-centimeter (0.125-inch) outside diameter surgical tubing which was much lighter and more flexible than regular Tygon tubing. A disadvantage of using surgical tubing was that it had to be replaced after every two flights because of deterioration.

### Balancing

To balance the probe on the rotating shaft, it was necessary to make the tail fins as light as possible while maintaining their strength. During the balancing, it was desirable to keep the mass and side area proportions between the forward and aft portions of the probe about the same. To accomplish this, the aft portion of the probe was hollowed out as much as possible and the tail fins were made out of titanium in the form of a hollow wedge (fig. 6).

### Limit Stops

If the probe was not positioned near the surface during takeoff or landing, full

---

<sup>1</sup>Since this study was made, a potentiometer has been developed (but not yet demonstrated in flight) that completely eliminates the flexible tubing from the rotational portion of the probe. Thus heavier tubing or hard lines can be used between the potentiometer and the transducer. Other problems such as tubing deterioration and kinking are also eliminated.

rotation would occur causing the surgical tubing to kink. To prevent this, limit stops were added between the potentiometer and drive screw to limit the probe rotation to approximately  $\pm 30^\circ$  throughout the probe traverse.

## SAMPLE PROFILES

Typical boundary-layer velocity profiles with flow angles for two consecutive traverses are presented in figure 7 for free-stream Mach numbers of 0.8, 1.6, and 2.0. Because this study was designed to flight test and demonstrate a pivoting traversing probe, the data are evaluated only in terms of the capability of the probe to measure incremental differences in the flow conditions through the boundary layer. Thus the results are not analyzed or interpreted in terms of the boundary-layer characteristics.

The data for Mach 0.8 (fig. 7(a)) show that the velocity ratios and flow angles for the two traverses differ. The differences in probe angle occur as a result of intentional airplane angle-of-attack changes during the data run, as mentioned previously. These changes in angle of attack also slightly changed the boundary-layer shape ( $u/u_e$ ) at this Mach number. The data show flow angle variations of about  $-0.5^\circ$  to about  $-1.8^\circ$  through the boundary layer.

The data for Mach 1.6 (fig. 7(b)) show that the boundary-layer shape ( $u/u_e$ ) did not change for both traverses, whereas the flow angles show some differences through the boundary layer. In this instance the flow angle variations ranged from about  $-2.3^\circ$  to  $0.9^\circ$  for most of the data. An example which shows that the pivoting traversing probe data are consistent with the reference probe data is included in the figure.

The data for Mach 2.0 (fig. 7(c)) again show that the velocity ratios for the two traverses are in good agreement but the flow angles ranged from  $0^\circ$  to approximately  $-1.2^\circ$ . The differences are again attributed to the changing airplane angle of attack.

The capability of the pivoting traversing probe to measure small variations in the flow conditions while traversing the boundary layer would be useful in defining the boundary layer adequately in areas where crossflow or mixed flows exist.

## CONCLUDING REMARKS

A prototype pivoting traversing probe was tested and evaluated in flight at Mach numbers of 0.8, 1.6, and 2.0. The unit was not optimized for size and weight but did successfully demonstrate the practicality of simultaneously measuring the flow angularity and pitot pressure through the boundary layer.

Flight Research Center  
National Aeronautics and Space Administration  
Edwards, Calif., January 28, 1974

## REFERENCES

1. Weidinger, Hanns: Drag Measurements on a Junkers Wing Section. NACA TM No. 428, 1927.
2. Bicknell, Joseph: Determination of the Profile Drag of an Airplane Wing in Flight at High Reynolds Numbers. NACA Rept. No. 667, 1939.
3. Roberts, Sean C.: A Flight Investigation of Profile Drag Measurements. Res. Note No. 16, Mississippi State Univ., Dec. 15, 1962.
4. George-Falvy, Dezso: Scale Effect Studies of Airfoil Profile Drag at High Subsonic Speed. AIAA Paper No. 71-289, 1971.
5. Saltzman, Edwin J.: In-Flight Use of Traversing Boundary-Layer Probes. NASA TN D-6428, 1971.
6. Mertaugh, Lawrence J., Jr.: In-Flight Comparisons of Boundary-Layer and Wake Measurement Probes for Incompressible Flow. NACA CR-127488, 1972.
7. Mechtly, E. A.: The International System of Units — Physical Constants and Conversion Factors. Second Revision. NASA SP-7012, 1973.
8. Lamb, J. P., Jr.: The Influence of Geometry Parameters Upon Lag Error in Airborne Pressure Measuring Systems. Tech. Rep. 57-351, Wright Air Dev. Center, U.S. Air Force, July 1957.

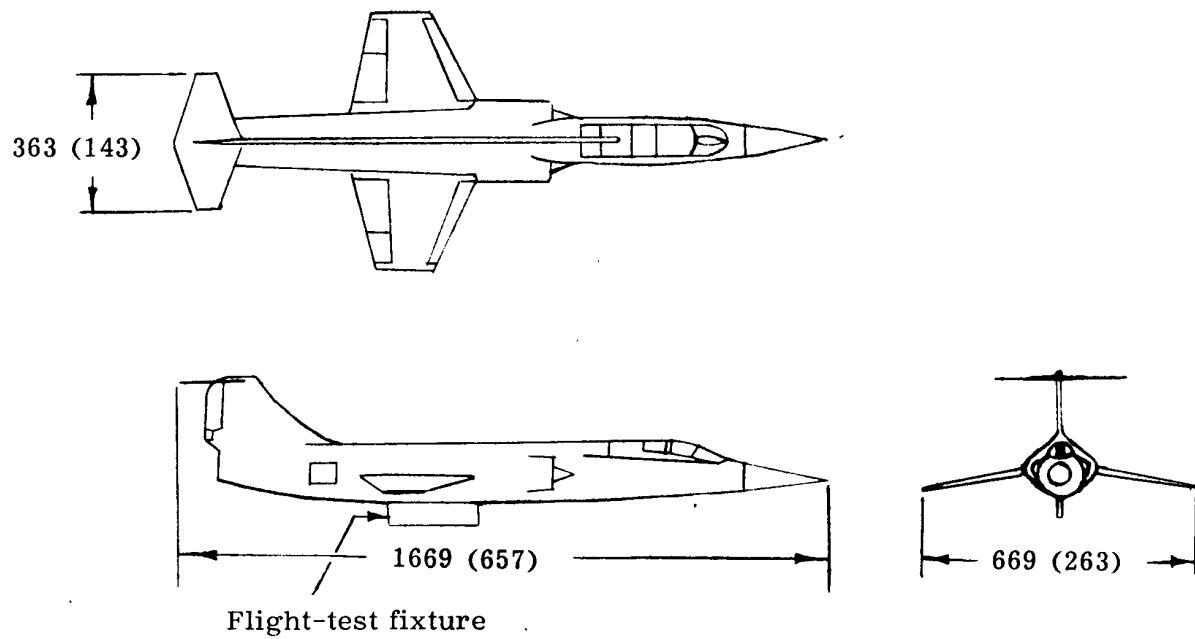


Figure 1. Sketch of F-104 airplane with flight-test fixture installed. Dimensions in centimeters (inches).



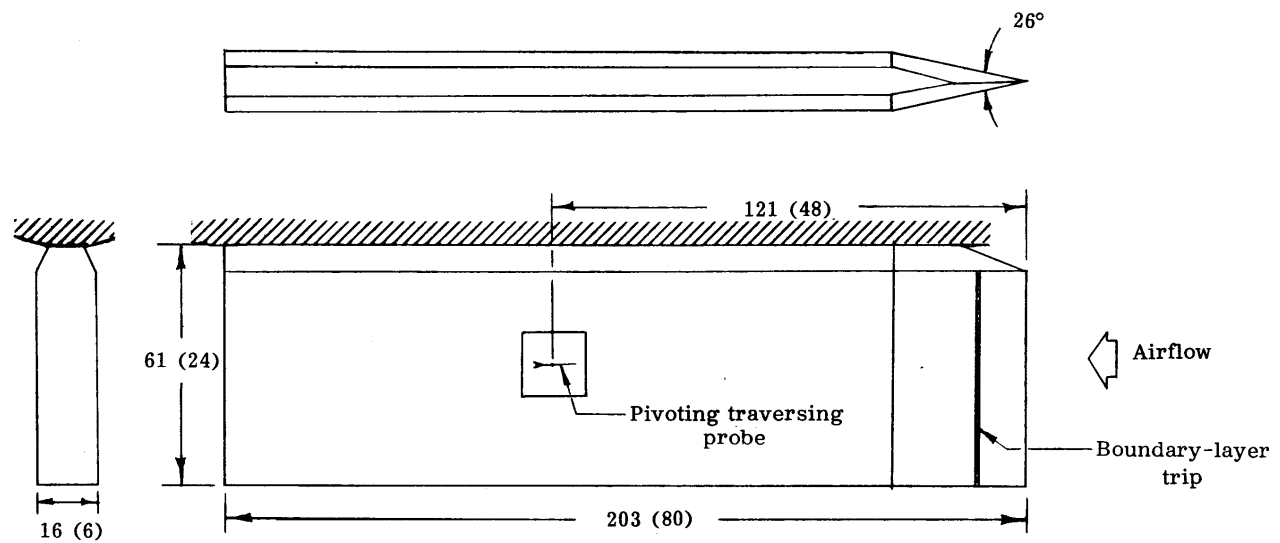


Figure 2. Three-view sketch of the flight-test fixture. Dimensions in centimeters (inches) unless otherwise indicated.

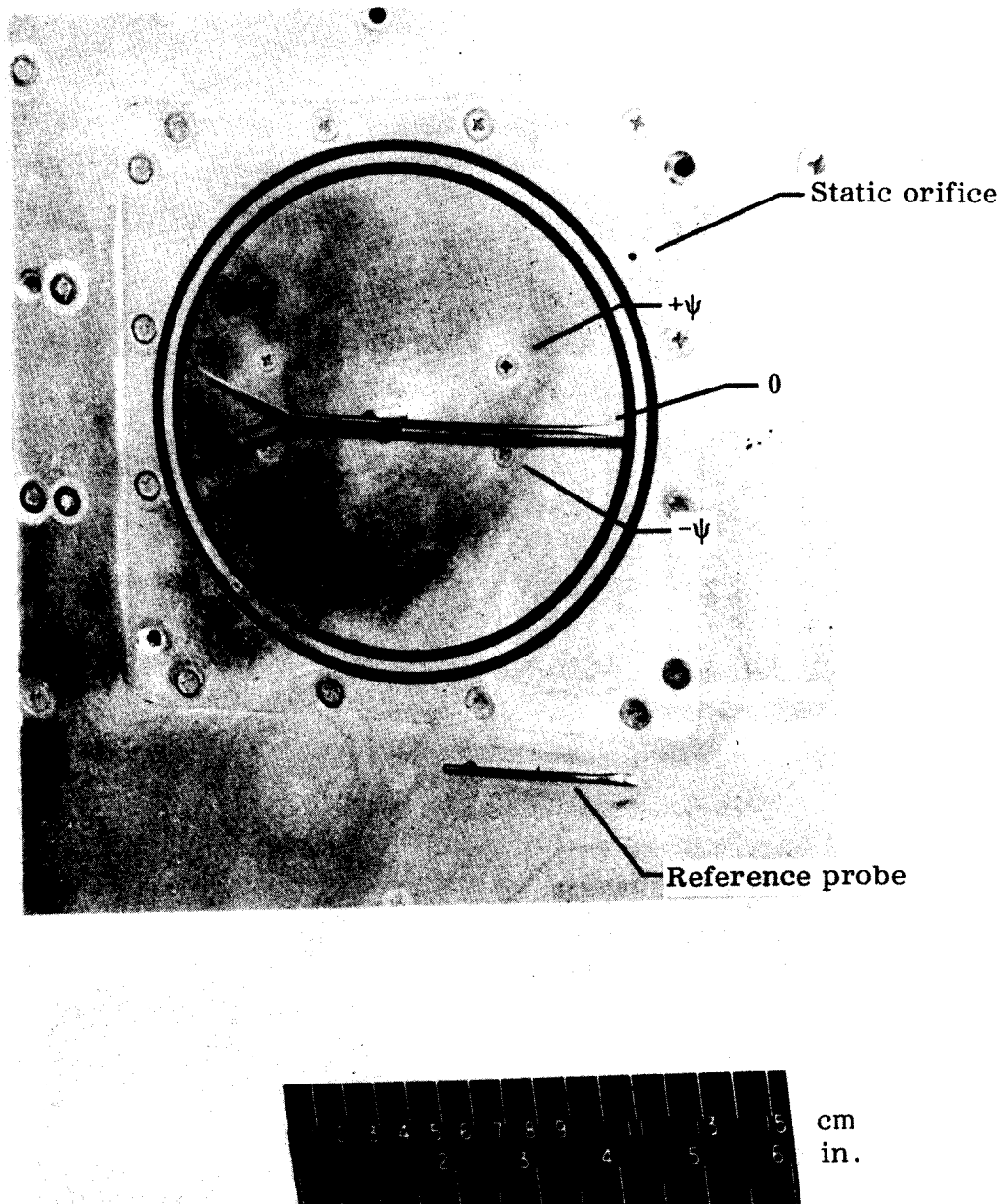


Figure 3. Pivoting traversing probe installed on the flight-test fixture with reference probe and static orifice.

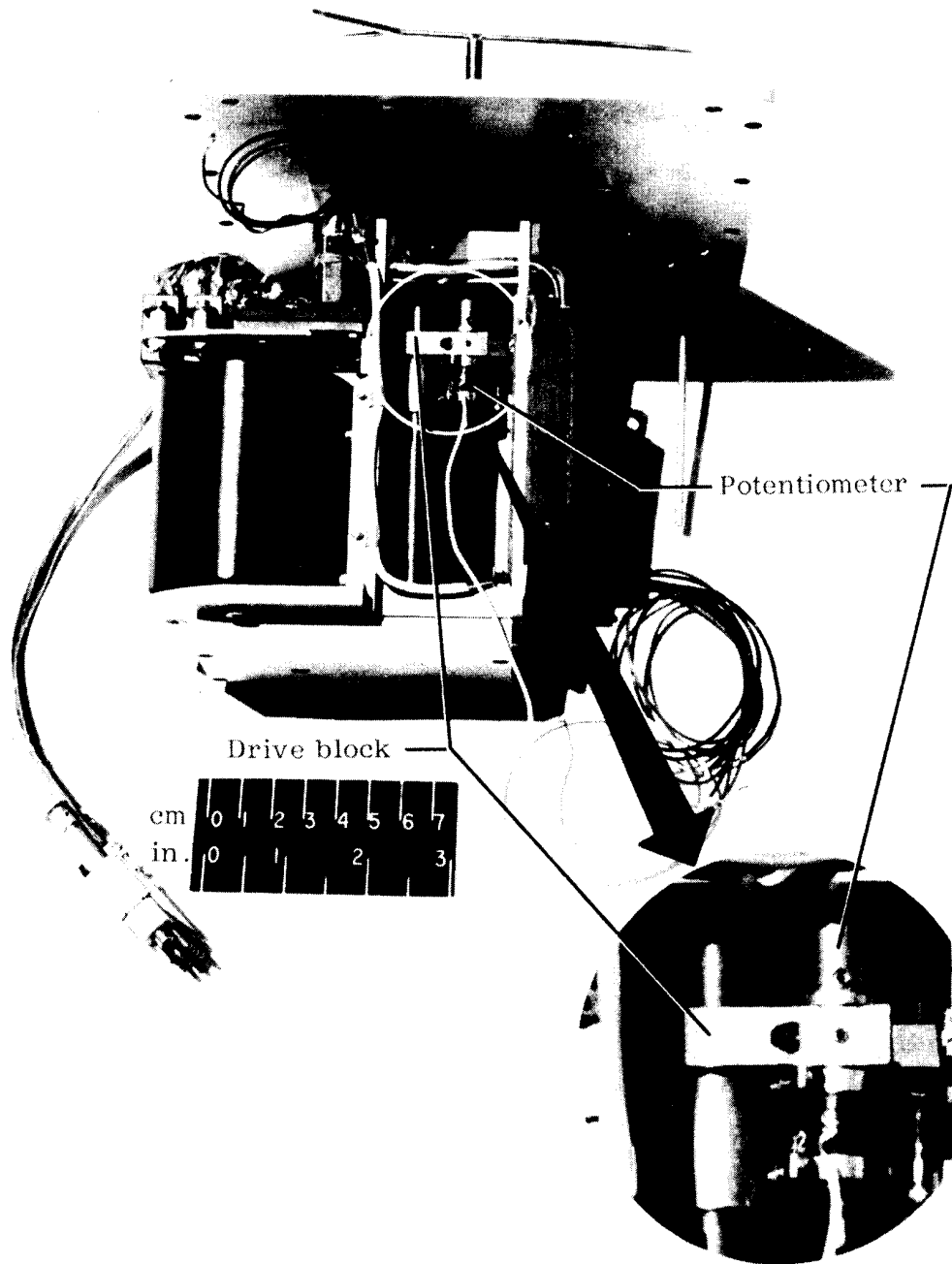


Figure 4. Complete pivoting traversing probe unit.

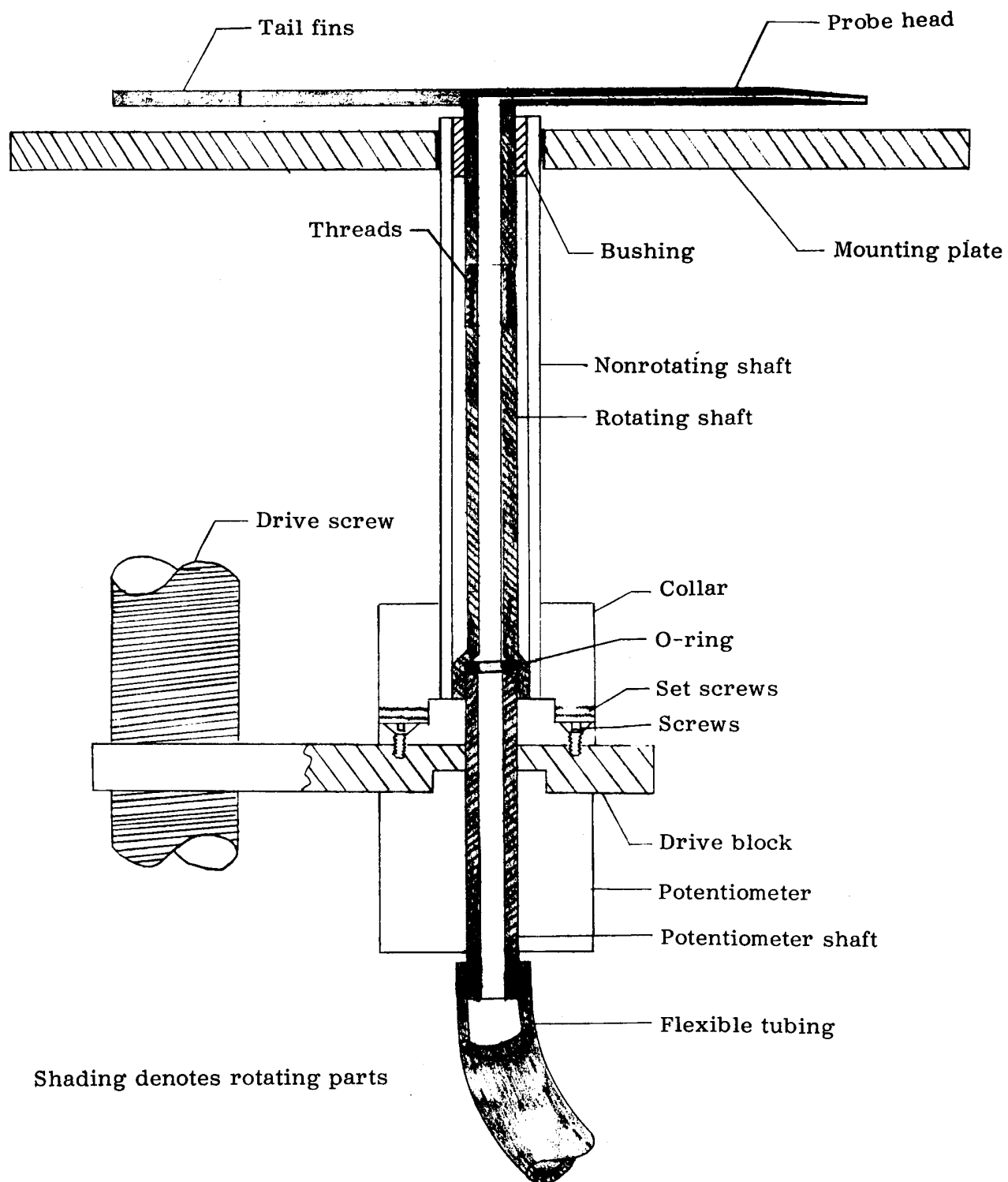


Figure 5. Schematic showing how pivoting traversing probe was constructed.

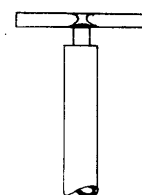
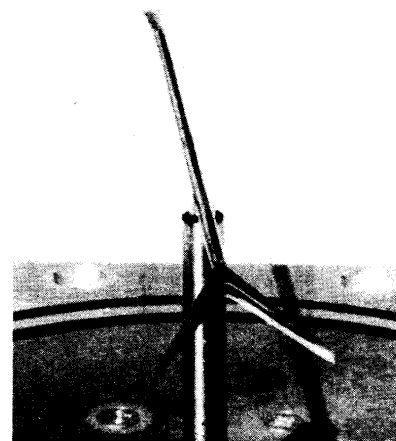
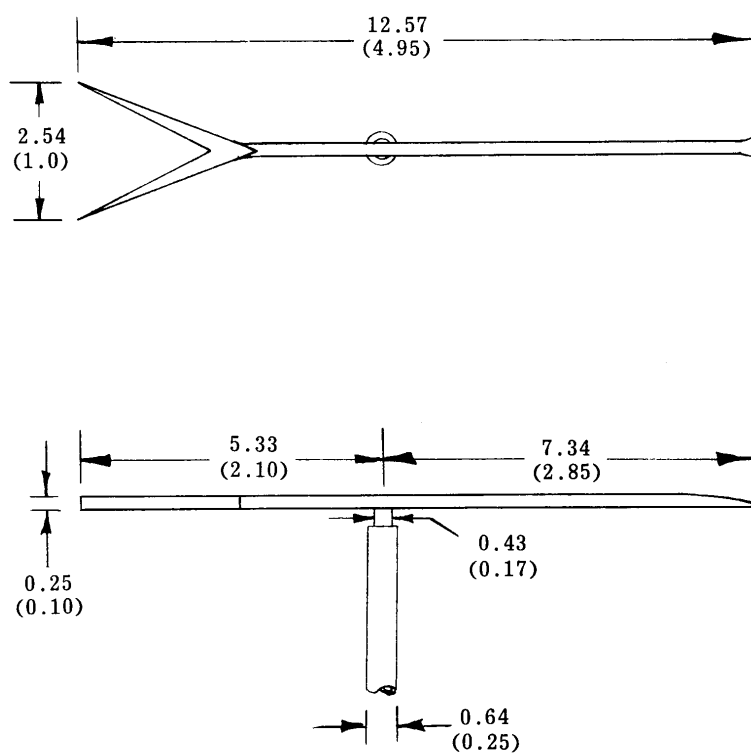
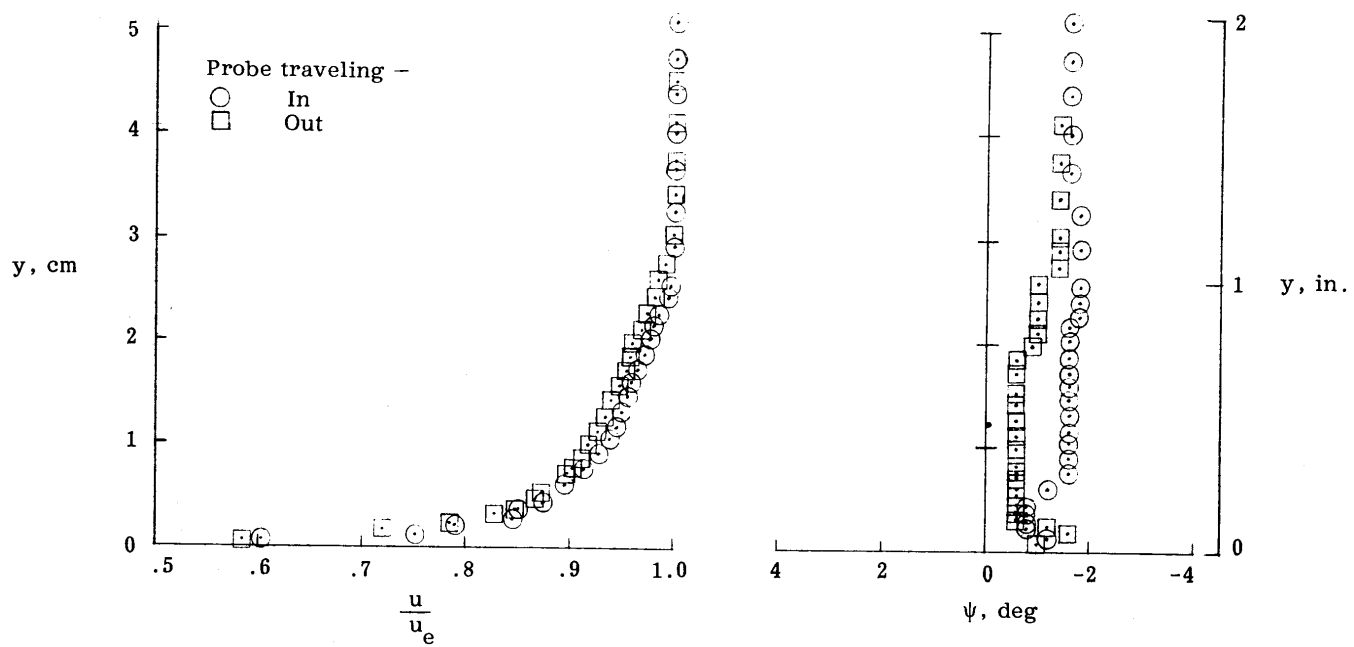
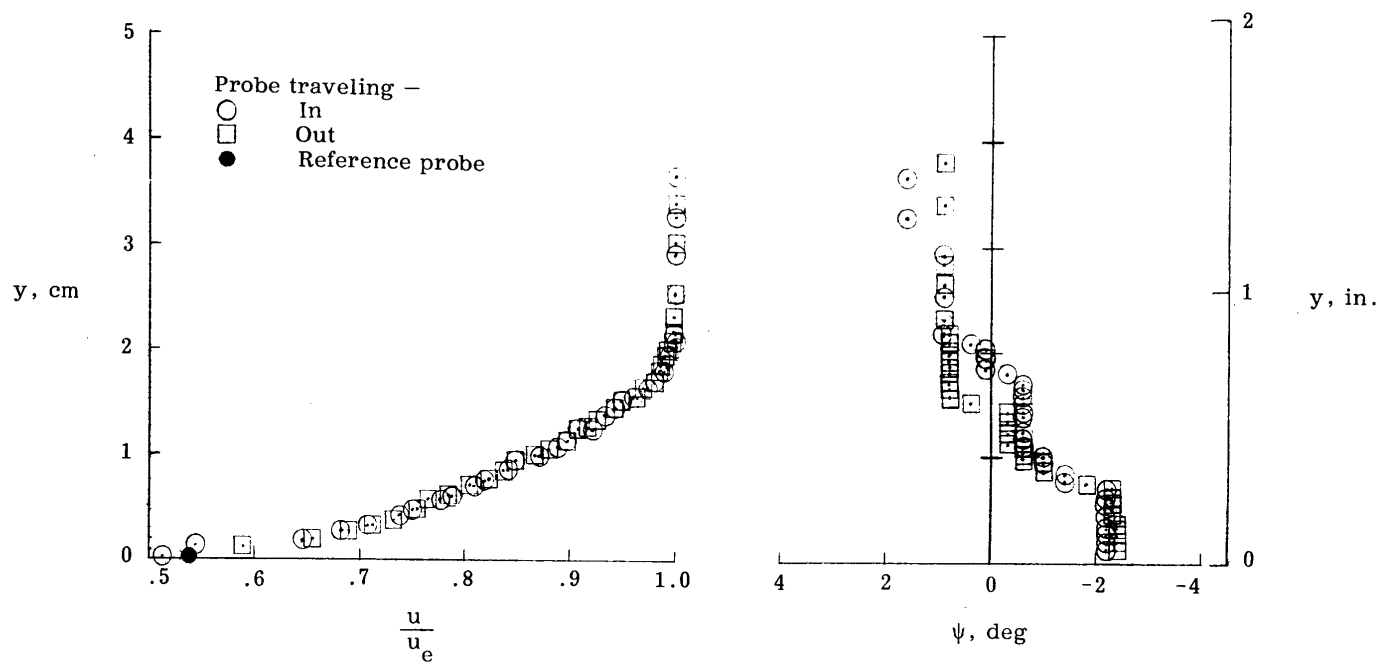


Figure 6. Probe head. Dimensions in centimeters (inches).



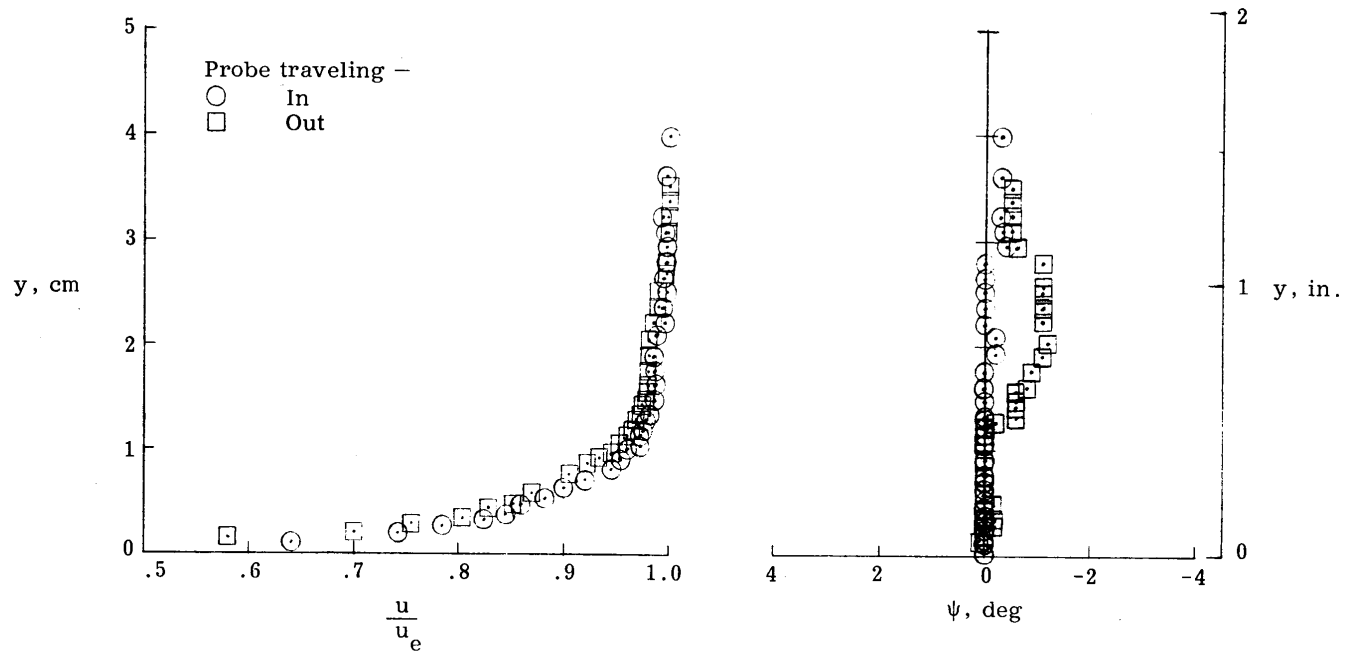
(a)  $M = 0.8$ .

Figure 7. Typical boundary-layer velocity profiles with flow angles.



(b)  $M = 1.6$ .

Figure 7 - Continued.



(c)  $M = 2.0$ .

Figure 7 - Concluded.